Computer modelling of $BaLiF_3$: II. Defects produced by divalent dopants

Computer modelling of BaLiF$_3$: II. Defects produced by divalent dopants

M E G Valerio†, R A Jackson‡ and J F de Lima†

† Departamento de Física, CCET, UFS, 49.100-000 São Cristóvão SE, Brazil
‡ Department of Chemistry, Keele University, Keele, Staffordshire ST5 5BG, UK

Abstract.   A computational study of the doping of BaLiF$_3$ by divalent ions (Pb^{2+}, Ni^{2+} and Co^{2+}) is presented. The calculations provide information on the energies involved in the doping process, and the consequent lattice relaxation. Predictions of the sites occupied by the dopant ions are made, which are supported by experimental results.

1. Introduction

BaLiF$_3$ is of interest as a potential laser material when doped with divalent cations. It has been shown, by Prado *et al* [2], that, when doped with Pb^{2+}, a new emission band in the near-infrared region is created which is broader than in other related materials when similarly doped. Similarly, in Ni^{2+} doped samples, Martins *et al* [3] observed that the material shows very good optical properties, in that the absorption of the main transition band overlaps the strong Nd emission line, with emission in the region around 1500 nm. This indicates promising applications as a tuneable laser in the near-infrared region, with potential uses in telecommunications. Similar properties were found in Co^{2+} doped samples by Duarte *et al* [4]. However, the positions adopted by the dopant ions in the BaLiF$_3$ matrix are not known, and the present paper will use computer modelling to investigate this.

Computer modelling provides a useful means of studying how the properties of BaLiF$_3$ are affected by such doping. A previous paper [1] has considered the problem of modelling perfect lattice properties and point defect behaviour in the material. This included calculations of formation energies for point defects, intrinsic defect formation and ion migration. In the present paper computer modelling will be used to study the doping of BaLiF$_3$ by Pb^{2+}, Co^{2+} and Ni^{2+} ions. Information will be obtained as to which sites in the lattice are preferentially occupied by these ions, and this will be compared with results of recent experimental studies on the doped material.

2. Computational method

2.1. Energy minimization and interionic potentials

The basic technique used in the work presented in this paper is lattice energy minimization, with interactions between ions represented by effective interionic potentials. For the host material, BaLiF$_3$, these potentials were fitted to experimental data, as described in the previous paper [1]. The present paper is concerned with doping the host material with

divalent cations, so potentials are needed to describe the interactions between the host ions and these cations. These were obtained by empirical fitting to the PbF_2, CoF_2 and NiF_2 structures, using the F–F potential obtained for $BaLiF_3$. Parameters are given in table 1.

Table 1. Potential parameters for dopant cation–F interactions.

Interaction	A (eV)	ρ (Å)
Pb_{core}–F_{shell}	400.0	0.4115
Co_{core}–F_{shell}	1613.5	0.2668
Ni_{core}–F_{shell}	1599.7	0.2628

2.2. Modelling of defects

In the previous paper [1] the method used for modelling intrinsic defects is described. The same method is used for the dopant cations (extrinsic defects), namely the Mott–Littleton approach [5]. Consistent region I and IIA radii were used (10 and 15 Å respectively) and a short-range cut-off of 10 Å was employed. The GULP program was used for all calculations [6].

3. Results

In considering the possible sites in the $BaLiF_3$ lattice where the dopant ions might substitute, attention must be paid to the problem of conservation of charge. If an M^{2+} cation substitutes at a Ba^{2+} site, then the charge is conserved. If however it substitutes at a Li^+ site, then there will be an excess of positive charge in the lattice which must be compensated. This charge compensation can take place in a number of ways, including the following:

(i) formation of a Li^+ vacancy;
(ii) formation of a F^- interstitial;
(iii) formation of a Ba^{2+} vacancy (compensates for two substitutions);
(iv) Li^+ substitution at a Ba^{2+} site.

Calculations have been performed for all the above possibilities, plus substitution at a Ba^{2+} site, for Pb^{2+}, Co^{2+} and Ni^{2+}. It should be noted that for mechanisms (i), (ii) and (iii), different non-equivalent symmetries were considered. For mechanism (i), there are three different configurations depending on the relative position of the Li^+ vacancy in relation to the substitutional M^{2+} ion: they can either be in face sharing $(-++)$, edge sharing $(--+)$ or corner sharing $(---)$ cubes. For mechanism (ii) there are three possible sites for the F^- interstitial: the centre of the edge of the Ba^{2+} cube $(0.5, 0, 0)$, the centre of the edge of the F^- octahedron $(0.5, 0.25, 0.25)$, and the midpoint of the diagonal of the Ba^{2+} cube between a Ba^{2+} and Li^+ ion $(0.25, 0.25, 0.25)$. For mechanism (iii) similar configurations were considered, with the two M^{2+} cations in either face $(-++)$, edge $(--+)$ or corner sharing $(---)$ cubes. All the above configurations can be seen in figure 1.

In each case, the following energies have been calculated, where appropriate:

(a) defect formation energies (E_f);
(b) defect binding energies (E_b) (the difference between the formation energy of a defect cluster and the sum of the formation energies of the isolated defects);
(c) solution energies (E_s) (the total energy for the substitution process)—see reactions in table 2.
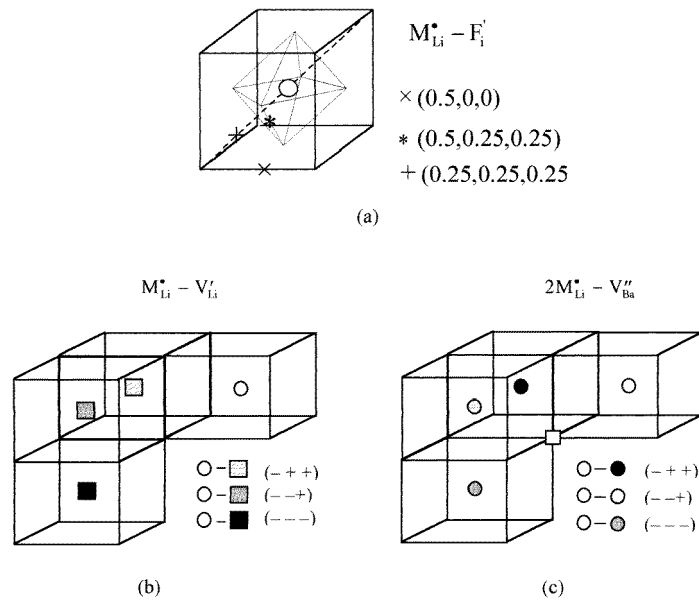
Figure 1. Symmetries of some impurity defects. Circles represent substitutional impurities; cross, star and plus represent F'_i; squares represent either Li or Ba vacancies. (a) Different arrangements of the F'_i in the $M^{\bullet}_{Li}$–F'_i defect. (b) Three possibilities of arranging the $M^{\bullet}_{Li}$ and the Li'_V in the $M^{\bullet}_{Li}$–Li'_V. (c) Configurations of the $2M^{\bullet}_{Li}$ in the $M^{\bullet}_{Li}$–V''_{Ba}.

Table 2. Reactions for solution of dopants in BaLiF$_3$.

Mechanism	Reaction
(i)	$MF_2 + Ba_{Ba} \leftrightarrow M_{Ba} + BaF_2$
(ii)	$MF_2 + 2Li_{Li} \leftrightarrow M^{\bullet}_{Li} + V'_{Li} + 2LiF$
(iii)	$MF_2 + Li_{Li} \leftrightarrow M^{\bullet}_{Li} + F'_i + LiF$
(iv)	$2MF_2 + 2Li_{Li} + Ba_{Ba} \leftrightarrow 2M^{\bullet}_{Li} + V''_{Ba} + BaF_2 + 2LiF$
(v)	$MF_2 + Li_{Li} + Ba_{Ba} \leftrightarrow M^{\bullet}_{Li} + Li'_{Ba} + BaF_2$

Table 3. Lattice energies of the metal fluorides.

System	$E_{lattice}$ (eV)
BaF$_2$	-23.13
LiF	-10.17
PbF$_2$	-22.35
CoF$_2$	-28.64
NiF$_2$	-29.29

The formation energies of the basic defects, namely V'_{Li}, V''_{Ba}, F'_i and Li'_{Ba}, used to calculate the binding energies of the impurity defects were the ones calculated in the previous paper [1]. The lattice energies of the metal fluorides used to calculate the solution energies are listed in table 3.

It is noted that the solution energy is the property whose magnitude will decide which

defect will be formed preferentially on energetic grounds. Similarly, the binding energy will indicate if a given defect cluster will be formed instead of the isolated defects. Tables 4, 5 and 6 contain, respectively, values of E_f, E_b and E_s.

Table 4. Defect formation energies.

Defect		E_f (eV)		
		Pb	Co	Ni
M_{Ba}		2.13	−3.15	−3.29
$M^\bullet_{Li}$		−3.65	−15.03	−15.80
$M^\bullet_{Li}$–V'_{Li}	$(-++)$	4.48	−6.99	−7.77
	$(--+)$	4.36	−7.11	−7.88
	$(---)$	4.23	−7.21	−7.98
$M^\bullet_{Li}$–F'_i	$(0.5, 0.0, 0.0)$	−6.10	−16.35	−17.11
	$(0.5, 0.25, 0.25)$	−6.09	−16.86	−17.53
	$(0.25, 0.25, 0.25)$	−4.68	−16.17	−16.90
$2M^\bullet_{Li}$–V''_{Ba}	$(-++)$	9.02	−12.40	−13.84
	$(--+)$	8.30	−12.44	−13.88
	$(---)$	8.34	−12.27	−13.71
$M^\bullet_{Li}$–Li'_{Ba}		5.87	−4.70	−5.43

Table 5. Defect binding energies.

Defect		E_b (eV)		
		Pb	Co	Ni
$M^\bullet_{Li}$–V'_{Li}	$(-++)$	−0.38	−0.47	−0.48
	$(--+)$	−0.50	−0.59	−0.59
	$(---)$	−0.63	−0.69	−0.69
$M^\bullet_{Li}$–F'_i	$(0.5, 0.0, 0.0)$	−1.98	−0.86	−0.85
	$(0.5, 0.25, 0.25)$	—	—	—
	$(0.25, 0.25, 0.25)$	−0.22	−0.29	−0.33
$2M^\bullet_{Li}$–V''_{Ba}	$(-++)$	−1.27	−0.74	−0.70
	$(--+)$	−1.63	−0.77	−0.72
	$(---)$	−1.61	−0.68	−0.63
$M^\bullet_{Li}$–Li'_{Ba}		−1.94	−1.13	−1.09

4. Conclusions

The most important point to be discussed is the question of which site is occupied by each ion, and which type of charge compensation, if needed, occurs. For Pb^{2+}, the site favoured is the Ba^{2+} position, so no charge compensation is required. For Co^{2+} and Ni^{2+}, the favoured site is the Li^+ position, with charge compensation achieved by the Li^+ ion moving to a Ba^{2+} site or by a Li^+ vacancy in the configuration of the $M^\bullet_{Li} + V'_{Li}$ $(---)$ complex. The binding energies show that both the $M^\bullet_{Li} + Li'_{Ba}$ and the $M^\bullet_{Li} + V'_{Li}$ complexes are bound, indicating that the charge compensation is local.

At first sight, this result is surprising, but it is supported by experimental evidence. At the time of carrying out the calculations, optical spectroscopy measurements were available that indicated an octahedral environment for Ni^{2+} [3]. Prompted by these calculations,

Table 6. Solution energies.

Defect		E_s (eV)		
		Pb	Co	Ni
M_{Ba}		1.35	2.36	2.87
$M^{\bullet}_{Li}$–V'_{Li}	$(-++)$	6.49	1.31	1.18
	$(--+)$	6.37	1.19	1.07
	$(---)$	6.24	1.09	0.97
$M^{\bullet}_{Li}$–F'_i	$(0.5, 0.0, 0.0)$	6.08	2.12	2.01
	$(0.5, 0.25, 0.25)$	6.09	1.61	1.59
	$(0.25, 0.25, 0.25)$	7.50	2.30	2.22
$2M^{\bullet}_{Li}$–V''_{Ba}	$(-++)$	5.13	1.41	1.26
	$(--+)$	4.77	1.37	1.12
	$(---)$	4.79	1.54	1.15
$M^{\bullet}_{Li}$–Li'_{Ba}		5.09	0.81	0.73

however, EXAFS measurements were carried out on a Ni-doped sample which indicate clearly that Ni^{2+} substitutes at the Li^+ position [7]. It is interesting to analyse the results in terms of the amount of relaxation induced in the lattice by these dopants. Table 7 shows the mean distances from the Ni^{2+} substitutional to the ions in the first, second, third and fourth shells in the case of $M^{\bullet}_{Li} + Li'_{Ba}$ and the $M^{\bullet}_{Li} + V'_{Li}$ $(---)$ complexes compared with the results obtained by Chadwick *et al* [7]. From these results we can conclude that both complexes could account for the displacements observed by EXAFS, thus confirming that Ni^{2+} would be in an octahedral environment. These results can also be understood if we consider that in both NiF_2 and CoF_2 the metals are located in a octahedral site surrounded by six F^- ions.

Table 7. Mean distances (in Å) from $Ni^{\bullet}_{Li}$ to first, second, third and fourth neighbour shells in $Ni^{\bullet}_{Li}$–Li'_{Ba} and $Ni^{\bullet}_{Li}$–V'_{Li} in $(---)$ defects compared with the mean distances obtained by EXAFS [7].

Neighbour shell	$Ni^{\bullet}_{Li}$–Li'_{Ba}	$Ni^{\bullet}_{Li}$–V'_{Li} $(---)$	EXAFS mean distance
1st	1.99	2.00	1.977 ± 0.002
2nd	3.56	3.55	3.554 ± 0.005
3rd	4.10	4.10	4.1 ± 0.1
4th	4.45	4.45	4.486 ± 0.007

In conclusion, the paper shows that computer modelling can predict the sites occupied by divalent dopant ions in $BaLiF_3$, producing results in agreement with experiment, including measurements carried out in direct response to the results of modelling.

Acknowledgments

References

[1] Jackson R A, Valerio M E G and de Lima J F 1996 *J. Phys.: Condens. Matter* **8** 10 931–7
[2] Prado L, Vieira N D Jr, Baldochi S L and Morato S P 1993 *Solid State Commun.* **87** 41–6
[3] Martins E, Vieira N D Jr, Baldochi S L and Morato S P 1994 *J. Lumin.* **62** 281–9
[4] Duarte M, Martins E, Baldochi S L, Vieira N D Jr and Vieira M M F 1995 *Pesq. Desenv. Tecnol. (BR)* **19** 24–5
[5] Mott N F and Littleton M J 1938 *Trans. Faraday Soc.* **34** 485
[6] Gale J D 1992–1996 *General Utility Lattice Program (GULP)* (Royal Institution of GB/Imperial College)
[7] Chadwick A V, Davis S R, Valerio M E G, de Lima J F and Baldochi S L 1996 *J. Phys.: Condens. Matter* **8** 10 697